

## Strength and Ductility of Concrete Encased Composite Beams

**Dr. Ammar A. Ali**

Building and Construction Engineering Department, University of Technology/Baghdad  
Email: ammarbagh@yahoo.com

**Saad N. Sadik**

Building and Construction Engineering Department, University of Technology/Baghdad

**Dr. Wael S. Abdul-Sahib**

Building and Construction Engineering Department, University of Technology/Baghdad

Received on: 25/9/2011 & Accepted on: 1/3/2012

### ABSTRACT

Experimental research was conducted to investigate the structural behavior of concrete-encased composite beams. Specimens were tested under lateral loading. The test results indicate that the behavior and failure mode of the beam are greatly affected by the steel beam core. The beams showed highly ductile behavior. The design flexural strength of concrete-encased beams is calculated from both the elastic and plastic stress distribution on the composite section. The deflection at the mid-span of the beam cannot be well predicted using linear elastic theory.

**Keywords:** Composite, beam, encased, strength

### مقاومة و لدونة العتبات المركبة و المغلفة بالخرسانة

#### الخلاصة

تم إجراء فحوصات عملية لبحث التصرف الإنشائي للعتبات المركبة و المغلفة بالخرسانة حيث تم تحميل العينات بأحمال عرضية. نتائج الفحوصات اظهرت ان التأثير الغالب هو للعتبة الفولاذية الداخلية. كما ان العتبات اظهرت لدونة عالية خلال الفحص. تم حساب مقاومة الانحناء التصميمية للعتبات المركبة و المغلفة بالخرسانة عن طريق استخدام كل من توزيع الاجهادات المرنة و اللدنة على المقطع المركب. وجد كذلك ان الهطول في منتصف فضاء العتبة لا يمكن تقديره باستخدام نظرية المرونة الخطية.

### INTRODUCTION

Composite construction employs structural members that are composed of two materials: structural steel (rolled or built-up) and reinforced concrete. Examples of composite members shown in Fig. (1) include (a) concrete-encased steel section, (b) concrete-encased steel beams, (c) steel beams interactive with and supporting concrete slabs, and (d) concrete-filled steel columns. In contrast with classical structural steel design, which considers only the strength of the steel, composite design assumes that the steel and concrete work together in resisting loads. The inclusion of the contribution of the concrete results in more economical designs, as the required quantity of steel can be reduced. Composite beams can take several forms. One of these forms is consisting of beams encased in

concrete (Fig.1.b). This is a practical alternative when the primary fireproofing structural steel is to encase it in concrete and as well the contribution of concrete could be accounted to share in the strength of the beam [1].

Work on encased beams dates back to 1922 in the report of the National Physical Laboratory tests on filler joist panels [2]. Many researches followed for both fully and partially encased beams [3, 4, 5, and 6]. Two types of composite beams are addressed in AISC 2010, Chapter I [7]: fully encased steel beams which depend on the natural bond of concrete to steel for composite action and those beams with mechanical anchorage to the slab using headed stud shear connectors or other types of connectors (such as channels) which do not have to be encased.

The present study here is coming to look for applicability of this form in the construction process used in Iraq. This comes from the feasibility of this form and it may be just insertion of the steel beam in the slabs of different thicknesses including or excluding shear connectors to form hidden or projected beams. The advantages of composite beams are:

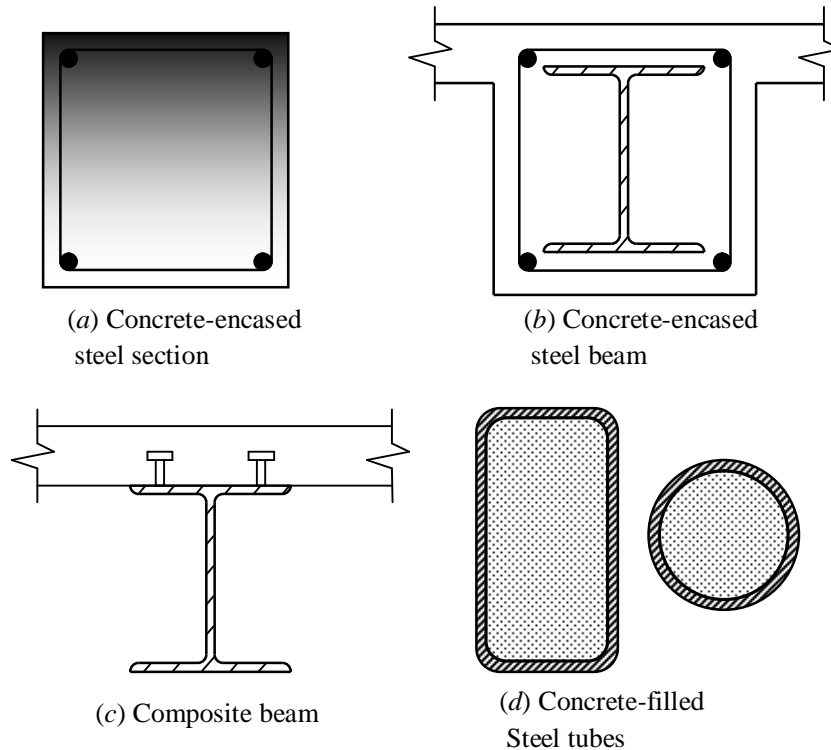


Figure (1) Composite sections

- Increased strength for a given cross sectional dimension.
- Good fire resistance in the case of concrete encased beams.
- Corrosion protection in encased beams.

- Significant economic advantages over either pure structural steel or reinforced concrete alternatives.
- Identical cross sections with different load and moment resistances can be produced by varying steel thickness, the concrete strength and reinforcement. This allows the outer dimensions of a beam to be held constant, thus simplifying the construction and architectural detailing.
- Concrete encased steel beams are also stronger in resisting impact loads.

**Test Specimens**

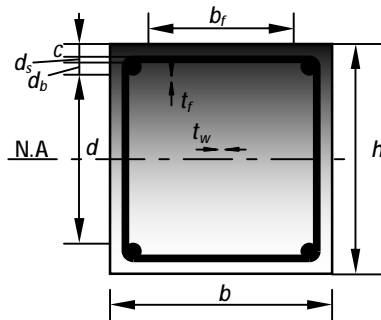
Two specimens were designed to represent a prototype beam used in medium-rise buildings. The test specimens had a square cross section of 150×150 mm and of 1.4 m span. Fig. (2) shows the configuration of the cross section. The test specimens consisted of the structural steel shape, longitudinal reinforcement, transverse reinforcement, and concrete.

The I-shaped structural steel used in the specimens is a hot-rolled section with material properties given in Table(1). The ratio of the structural steel area to the gross area was 3.6%. The centroids of both the structural steel shape and the geometric center of the beam cross section are coincident.

As shown in Fig.(2), a longitudinal bar was placed at each corner of the beam. The longitudinal bars were applied to tensile test and were of minimum yield strength of 592 MPa, 12 mm in diameter and deformed. In addition, cross ties of 6 mm in diameter were used to engage the longitudinal bars and to enhance the deformation ductility of the beam. The stirrups spacing was 160 mm center to center. The measured material strengths are given in Table(1).

**Steel Section**

- $d = 100 \text{ mm}$
- $b_f = 50 \text{ mm}$
- $t_f = 5.7 \text{ mm}$
- $t_w = 3 \text{ mm}$
- $F_y = 273.5 \text{ MPa}$



**RC Section**

- $h = 150 \text{ mm}$
- $b = 150 \text{ mm}$
- $d_s = 6 \text{ mm}$
- $c = 7 \text{ mm}$
- $d_b = 12 \text{ mm}$
- $A_b = 452.4 \text{ mm}^2$

Figure (2) Composite beam cross-section of test specimen.

**Table (1). Measured mechanical properties of structural steel and reinforcement.**

| Material      | Yield strength (MPa) | Ultimate strength (MPa) |
|---------------|----------------------|-------------------------|
| Steel         | 273.5                | 461                     |
| Rebar (12 mm) | 592                  | 680                     |

The concrete cube strength was 31.3 MPa, of three specimens measured at time of testing (28 days). The mix design for concrete is done depending on the American Concrete Institute (ACI) mix design method.

**TEST SETUP AND TEST PROCEDURE**

Fig.(3) is showing the test machine and Fig.(4) illustrates the test setup for simulating the loading state of a beam. Roller and hinge supports were used at ends of the specimen. With this test setup, the bending moment is peak at mid-span of the specimen.

The lateral load was applied by a hydraulic jack to the midpoint of the beam, using a load step of 5 kN.



**Figure (3) Test setup.**

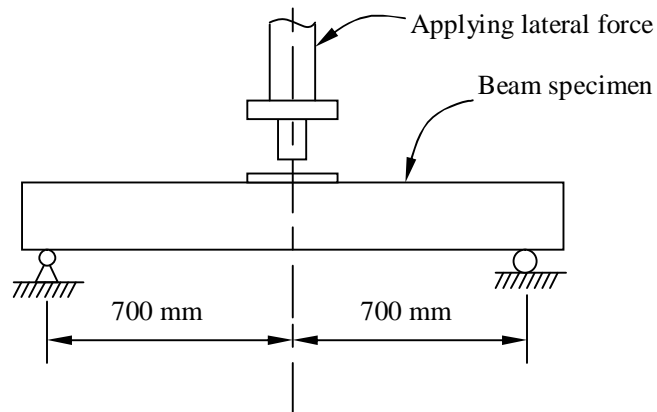


Figure (4) Schematics of test setup.

#### BEHAVIOR AND FAILURE MODE

For both specimens, flexural cracks initially occurred at load of 40 kN; afterwards, the cracks progressively grew as shown in Fig.(5). The response of the specimens is presented in the load–displacement curves of Figs.(8) and (9).

It can be seen that the beam is showing linear behavior until 60 kN load; afterwards, the nonlinearity of the curve began and the beam will behave plastically as a plastic hinge occurring at the mid-span at loads of 110 kN and 100 kN for specimens 1 and 2, respectively. Ductility of the beam is very high that because of the high percentage of steel area and this is one of the favorable features for seismic construction.

The failure in the concrete is first by cracking of the tension zone and later by crushing of the compression zone. The steel shape and reinforcement continue in the plastic region and high deflection will be produced. The failure phenomena were similar for both specimens.

#### ANALYSIS

The AISC LRFD Specification [7] permits two methods of design for encased steel beams. In the first method, the design strength of the encased section is based on the plastic moment capacity,  $\phi_b M_p$ , of the steel section alone. In the second method, the design strength of the encased section is based on the first yield of the tension flange assuming composite action of the concrete that is in compression and the steel section. Either way, there is no need to consider local buckling or lateral-torsional buckling of the steel beam because such buckling is inhibited.



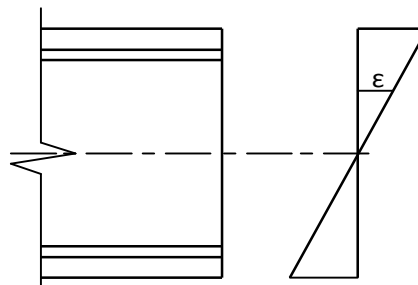
Figure (5) Flexural failure.

The properties of the section components are as given in Fig.(2).

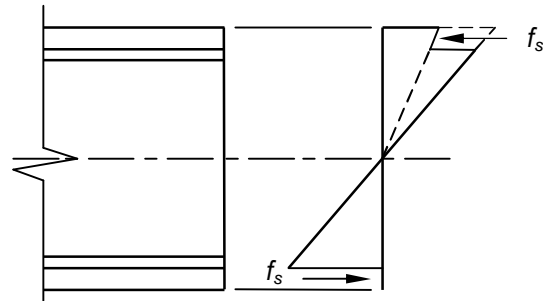
Concrete strengths are specified in terms of the characteristic cube strengths,  $f_{cu}$ , measured at 28 days. To convert to cylinder compressive strength  $f'_c$  a factor of 0.8 is used here.

It is used four 12 mm-diameter bars as longitudinal reinforcement of  $f_y = 592$  MPa and tied with undeformed 6 mm-stirrups.  $f_y$  is the yielding strength of the steel reinforcement bars.

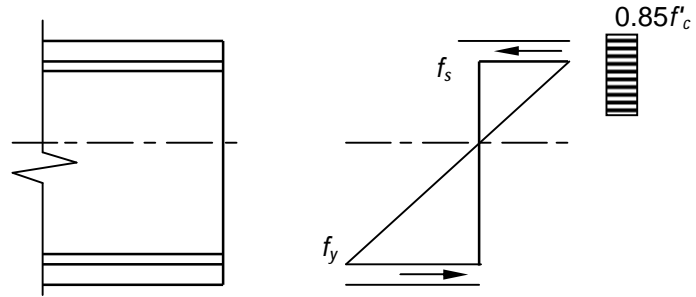
The distribution of internal normal strains and stresses on the cross section of a beam is shown in Fig.(5) assuming no slippage between steel and concrete [1]. It is based on the idealized stress-strain diagram for structural steel in Fig.(6), which is a simplified version of the actual stress-strain curves.



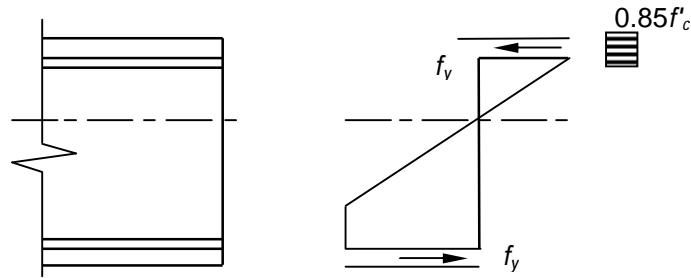
(a) Strain.



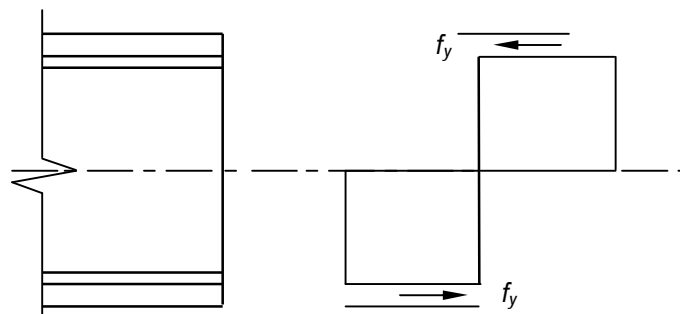
(b) Initial stresses



(c) Block stress in concrete



(d) Yielding of steel section and rebars



(e) Full yielding of steel section.

**Figure (6) Strains and stresses diagrams.**

As shown in Fig.(6), the normal strain distribution is always linear, neglecting the shear deformation effect. The magnitude of strain is proportional to the distance from the neutral (or centroidal) axis. On one side of the neutral axis, the fibers of the flexural member are in tension (or elongation); on the other side, in compression (or shortening). The distribution of normal stresses depends on the magnitude of the load. Under initial loads before yielding, stresses (which are proportional to strains in Fig. (6.a) are also linearly distributed on the cross section for both steel and concrete (Fig. 6.b). The strain will increase under additional load and this will lead concrete to behave nonlinearly and here stress block may be used to represent stresses in the concrete as shown in Fig. 6.c [10]. The maximum stress in steel, however, is the yield stress  $F_y$  (Fig. 6.d). Yielding will proceed inward, from the outer fibers to the neutral axis as shown in Fig.(6.e), as the load is increased, until a plastic hinge is formed. Forming plastic hinge will lead to crushing concrete in compression zone and the steel section will work alone. The idealized plastic behavior of structural steel is shown in Fig.(7).

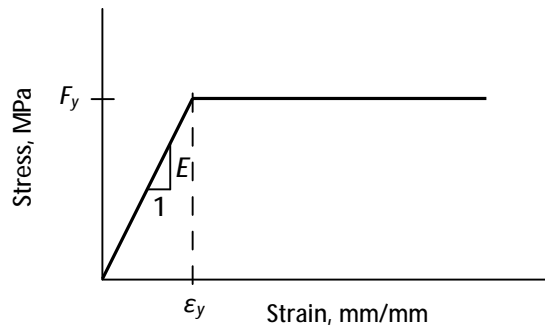


Figure (7) Idealized stress-strain diagram for structural steel.

Another relationship depending on BS 5400: Part 5, Appendix C [8] requirements that assume for concrete-encased section the plastic neutral axis will be within the flange [9]. This is illustrated in Fig.(8).

Only beams which are compact (i.e., not susceptible to local buckling) and adequately braced (to prevent lateral-torsional buckling) can attain this upper limit of flexural strength. The relationships between moment and maximum (extreme fiber) bending stresses, tension or compression, at a given cross section have been derived in a number of engineering mechanics textbooks. At the various stages of loading, they are as follows:

Until initial yielding:

$$M = Sf_b \quad \dots(1)$$



At initial yielding:

$$M_y = SF_y \quad \dots(2)$$

At full plastification (i.e., plastic hinge):

$$M_p = ZF_y \quad \dots(3)$$

Where

$M$  = bending moment due to the applied loads, N.mm.

$M_y$  = bending moment capacity at yielding, N.mm.

$M_p$  = full plastic moment capacity, N.mm.

$S$  = elastic section modulus,  $\text{mm}^3$ .

$Z$  = plastic section modulus,  $\text{mm}^3$ .

$f_b$  = maximum normal stress due to bending, MPa.

$F_y$  = specified minimum yield stress for steel section, MPa.

Elastic section modulus  $S = I / c$ .

Where  $I$  is the moment of inertia of the cross section about its centroidal axis; and  $c$  is the distance from the centroid to the extreme fiber.

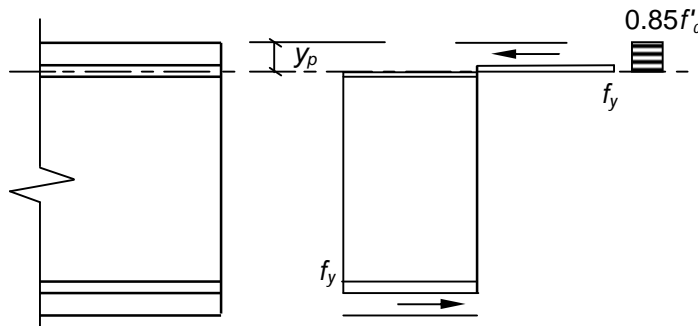


Figure (8) Stresses at plastification.

The total area of steel section  $A_s$  is,  $A_s = 835.8 \text{ mm}^2$ , and distance between the extreme face of the flange and location of center of area of upper half of steel section,  $\bar{y}_t$ , is:

$$\bar{y}_t = \frac{b_f t_f^2 + \frac{t_w}{4} (d^2 - 4t_f^2)}{A_s} \quad \dots (4)$$

$$\bar{y}_t = 10.8 \text{ mm}$$

$$a = 100 - 2 \times 10.8 = 78.4 \text{ mm}$$

$$Z = \frac{A_s}{2} a = 32763 \text{ mm}^3$$

$$M_p = F_y Z + 0.5 A_b f_y (h - d_r) \quad \dots(5)$$

Where

$f_y$  = yield strength of steel reinforcement.

$A_b$ = area of reinforcement.

$d_r$  = the cover to reinforcement.

For the moment strength of bare steel section as per AISC LRFD [7]:

$M_{p1}$  = 8.9 kN.m.

$P_{p1}$  = 25.6 kN.

The load strength  $P_{p1}$  which is so conservative compared with experimental load  $P_p$  = 98 kN. But, if the effect of reinforcement is included as in Eq.(5), the moment and load strengths will be:

$M_{p2}$  = 27.3 kN.m.

$P_{p2}$  = 75.6 kN.

The great effect of reinforcement in strength of the composite section could be noticed here.

Applying procedure as given by Davidson [9],

$$M_p = 0.5A_sF_y(h - y_p) + 0.5A_b0.87f_y(h - d_r) \quad \dots (6)$$

$M_{p3}$  = 26.4 kN.m.

$P_{p3}$  = 75.3 kN.

If assuming that the reinforcement in the top and bottom layers is fully yielded in Eq.(6):

$M_{p4}$  = 28.6 kN.m.

$P_{p4}$  = 81.8 kN.

In the above,  $M_{pi}$  is the moment strength and  $P_{pi}$  is the maximum center load,

$$P_{pi} = \frac{4M_{pi}}{L} \quad \dots (7)$$

The comparison above shows that using bare steel shape as recommended by AISC LRFD [7] will be very conservative for this case. Adding the effect of longitudinal reinforcement will enhance the prediction of the experimental load. This may be due to the high ratio of reinforcement for the 150×150 mm section which is 35% of the total steel area. Also the high yielding strength of reinforcement compared to the steel shape. British Standards (BS) procedure as presented by Davidson [9] is giving similar results, if longitudinal reinforcement is included. Results of procedure given by Davidson, assuming not full yielding of reinforcement, will be more close to the experimental results and difference will be 16% in the safe side. The comparison is given in Fig.(9).

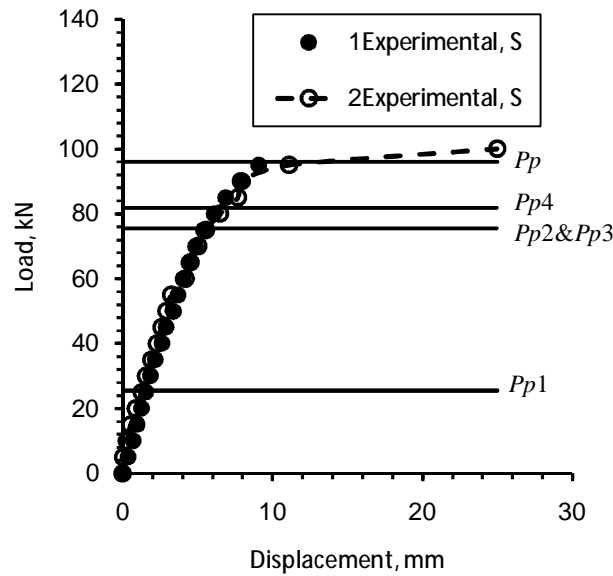


Figure (9) Ultimate strength comparison using Different methods.

**DEFLECTIONS**

Deflection is a serviceability limit state, not one of strength, so deflections should always be computed with service loads. The deflections due to loading applied to the composite beams shall be calculated using elastic analysis with the flexural stiffness equal to the mean value of  $E_s I_1$  and  $E_s I_2$ .  $E_s$  is the modulus of elasticity for structural steel,  $I_1$  is the second moment of area of the effective equivalent steel section assuming that concrete in tension is uncracked, and  $I_2$  is the second moment of area of the steel section only neglecting the concrete.

Computing  $I_1$  the moment of inertia about the  $x$ -axis of the whole beam,

$$I_1 = I_0 + A_s (y_b - y_s)^2 + \frac{1}{12} \left(\frac{b}{n}\right) h^3 + A_{c(trans)} (y_b - y_c)^2 \dots (8)$$

In this formula:

$I_0$  = moment of inertia of steel about its own axis,  $mm^4$ .

$b$  = width of section, mm.

$h$  = depth of section, mm.

$A_s$  = area of steel,  $mm^2$ .

$y_b$  = distance from the bottom of the beam to the neutral axis of the whole beam, mm.

$$y_b = \frac{A_s y_s + A_{c(trans)} y_c}{A_{total}}$$

$y_s$  = distance between the steel's neutral axis and the bottom of the beam, mm.

$A_{c(trans)}$  = transformed area of the concrete =  $hb / n$ ,

$y_c$  = distance between the neutral axis of the concrete and the bottom of the beam.

$E_c$  = modulus of elasticity of concrete, and

$n$  = modular ratio

$$n = \frac{E_s}{E_c}$$

The ACI 318-08 Building Code [10] gives the value of  $E_c$  as  $w_c^{1.5} \cdot 0.043 \sqrt{f'_c}$  (in MPa) for values of  $w_c$  between 1440 and 2560 kg/m<sup>3</sup> and for normal concrete it may be taken as  $4700 \sqrt{f'_c}$  where

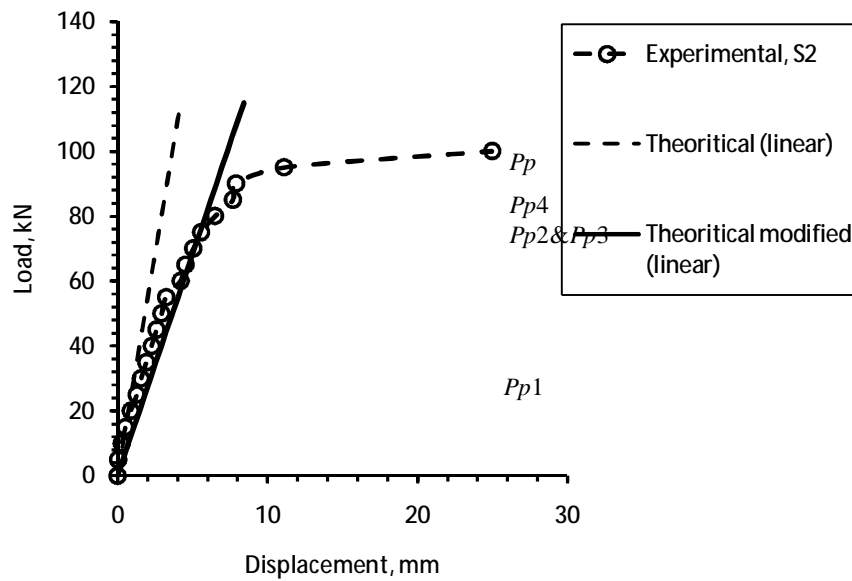


Figure (10) Load-displacement behavior.

$w_c$  = unit weight of concrete (kg/m<sup>3</sup>) (normal weight concrete weighs approximately 2400 kg/m<sup>3</sup>).

$f'_c$  = 28-day compressive strength of concrete (MPa).

Now applying the previous steps, having:

$b_f = 50$  mm,  $d = 100$  mm,  $t_f = 5.7$  mm,  $t_w = 3$  mm.

$h = 150$  mm,  $b = 150$  mm,  $c = 7$  mm,  $d_b = 12$  mm,  $d_t = 6$  mm.

$$f'_c = 25 \text{ MPa}, f_{y,bar} = 592 \text{ MPa}, F_y = 273.5 \text{ MPa}, E_s = 200\,000 \text{ MPa}.$$

$$E_c = 4700 \sqrt{f'_c} = 23\,500 \text{ MPa}.$$

$$n = \frac{E_s}{E_c} = \frac{200000}{23500} = 8.5.$$

$$A_s = 836 \text{ mm}^2, A_{c(trans)} = 2647 \text{ mm}^2.$$

$$A_{total} = 3483 \text{ mm}^2.$$

$$y_b = 75 \text{ mm}.$$

$$I_0 = 1424333 \text{ mm}^4.$$

$$I_1 = 6387568 \text{ mm}^4.$$

$$I_2 = I_0 = 1424333 \text{ mm}^4.$$

It can be seen from Fig. 10 that using the average modified stiffness of the section gave more close result to predict the behavior within the linear region than that of the uncracked section.

## CONCLUSIONS

Flexural tests were conducted to evaluate the structural behavior of the proposed composite beam using I-shape steel section with reinforced concrete encasement. The following conclusions were drawn from the results:

(1) The ultimate strength of the proposed system exceeded the design value. It failed due to concrete crushing in the compression zone without bond or local failure. This behavior was in accordance with the design objective, i.e., complete composite action before yield and partial composite action after yield. This design concept enabled the proposed system to develop sufficient ductility, strength, and consequently effective composite behavior, without causing serviceability problems.

(2) The flexural strength determined using the plastic stress distribution on the steel section for the limit state of yielding (plastic moment) as adopted by AISC LRFD is too conservative for the case of reinforced concrete encasement.

(3) It is found that considering the effect of the longitudinal reinforcement in the strength of the section important to get more close to experimental results.

(4) Using BS method as in [8] with fully yielded reinforcement will lead to strength as conservative as 16%.

(5) Deflection estimation using simplified method within the linear region is more accurate by using the modified flexural stiffness.

## REFERENCES

- [1] Rokach, A.J., Theory and Problems of Structural Steel Design, McGraw Hill, New York, NY., 1991.

- [2] Adekola, A.O., "Elastic and plastic behaviour of cased beams", Build. Sci. Vol.2, pp. 321-330, Pergamon Press 1968, Printed in Great Britain.
- [3] Kindmann, R. and Bergmann, R., "Effect of reinforced concrete between the flanges of the steel profile of partially encased composite beams", J. Construct. Steel Research, 27, 107-122, 1993.
- [4] Roeder, C.W., Chmielowski, and Brown, C.B., "Shear connector requirements for embedded steel sections", ASCE Journal of Structural Engineering, Vol. 125, No. 2, February, 1999.
- [5] Hegger, J. and Goralski, C., "Structural behavior of partially concrete encased composite sections with high strength concrete", In: Composite construction in steel and concrete V: proceedings of the 5th international conference, Structural Engineering Institute of the American Society of Civil Engineers. Reston, VA: American Society of Civil Engineers, 2006.
- [6] Elghazouli, A.Y. and Treadway, J., "Inelastic behaviour of composite members under combined bending and axial loading", Journal of Constructional Steel Research 64, 1008–1019, 2008.
- [7] AISC, Specification for Structural Steel Buildings, American Institute of Steel Construction, Chicago, IL., 2010.
- [8] British Standards Institution, Steel, concrete and composite bridges. Part 5: Code of practice for design of composite bridges. BS 5400, BSI, London, 1979.
- [9] Davison, B. and Owens, G.W. (Editors), "Steel Designer's Manual" 6th edition, Blackwell Scientific publications, Oxford, 2003.
- [10] ACI, Building Code Requirements for Structural Concrete (ACI 318M-08) and Commentary, Farmington Hills, MI., 2008.